

UCLA

UCLA Previously Published Works

Title

Altered Exosomal RNA Profiles in Bronchoalveolar Lavage from Lung Transplants with Acute Rejection

Permalink

<https://escholarship.org/uc/item/5jk5f6r2>

Journal

American Journal of Respiratory and Critical Care Medicine, 192(12)

ISSN

1073-449X

Authors

Gregson, Aric L
Hoji, Aki
Injean, Patil
et al.

Publication Date

2015-12-15

DOI

10.1164/rccm.201503-0558oc

Peer reviewed

Altered Exosomal RNA Profiles in Bronchoalveolar Lavage from Lung Transplants with Acute Rejection

Aric L. Gregson¹, Aki Hoji², Patil Injean³, Steven T. Poynter³, Claudia Briones³, Vyacheslav Palchevskiy³, S. Sam Weigt³, Michael Y. Shino³, Ariss Derhovanessian³, David Sayah³, Rajan Saggarr³, David Ross³, Abbas Ardehali⁴, Joseph P. Lynch III³, and John A. Belperio³

¹Division of Infectious Diseases, Department of Medicine, ³Division of Pulmonary, Critical Care, Allergy, and Immunology, Department of Medicine, and ⁴Division of Cardiothoracic Surgery, Department of Surgery, University of California, Los Angeles, California; and ²Department of Transplantation, University of Pittsburgh, Pittsburgh, Pennsylvania

ORCID IDs: 0000-0001-6806-0868 (A.L.G.); 0000-0001-7021-8273 (D.S.).

Abstract

Rationale: The mechanism by which acute allograft rejection leads to chronic rejection remains poorly understood despite its common occurrence. Exosomes, membrane vesicles released from cells within the lung allograft, contain a diverse array of biomolecules that closely reflect the biologic state of the cell and tissue from which they are released. Exosome transcriptomes may provide a better understanding of the rejection process. Furthermore, biomarkers originating from this transcriptome could provide timely and sensitive detection of acute cellular rejection (AR), reducing the incidence of severe AR and chronic lung allograft dysfunction and improving outcomes.

Objectives: To provide an in-depth analysis of the bronchoalveolar lavage fluid exosomal shuttle RNA population after lung transplantation and evaluate for differential expression between acute AR and quiescence.

Methods: Serial bronchoalveolar lavage specimens were ultracentrifuged to obtain the exosomal pellet for RNA extraction, on which RNA-Seq was performed.

Measurements and Main Results: AR demonstrates an intense inflammatory environment, skewed toward both innate and adaptive immune responses. Novel, potential upstream regulators identified offer potential therapeutic targets.

Conclusions: Our findings validate bronchoalveolar lavage fluid exosomal shuttle RNA as a source for understanding the pathophysiology of AR and for biomarker discovery in lung transplantation.

Keywords: exosome; rejection; lung; transplantation; RNA

Lung transplantation is the sole therapeutic option for end-stage lung disorders, but is complicated by allograft rejection with an incidence and severity that is among the highest of solid organ transplants (1). Long-term survival is dependent on recipients remaining free of chronic lung allograft

dysfunction (CLAD), of which there are two forms: an obstructive, fibroobliterative syndrome (bronchiolitis obliterans syndrome) (2), and a restrictive type (restrictive allograft syndrome, also known as restrictive-CLAD) (3). CLAD affects more than 60% of lung transplant

recipients within 5 years of transplantation and imparts a substantial 50% 3-year mortality (4).

Acute cellular rejection (AR) was among the first identified risk factors for CLAD (1), and is an alloimmune-driven process, involving both CD4 and CD8

(Received in original form March 19, 2015; accepted in final form August 26, 2015)

Supported by K23HL102220 and Cystic Fibrosis Foundation Pilot and Feasibility Grant (A.L.G.), HL112990 and CTOT 11532596 (J.A.B.), K23HL094746 and the Joyce and Saul Brandman Foundation Fund (S.S.W.), and the National Center for Advancing Translational Sciences through UCLA CTSI grant UL1TR000124.

Author Contributions: Conception, hypothesis, design, data collection, analysis, interpretation, manuscript writing/revision, A.L.G. Conception, design, analysis, interpretation, manuscript writing/revision, A.H. Data collection, analysis, interpretation, P.I., S.T.P., C.B., and V.P. Data collection, S.S.W., M.Y.S., A.D., D.S., R.S., D.R., A.A., and J.P.L. Interpretation, manuscript writing/revision, J.A.B.

Correspondence and requests for reprints should be addressed to Aric L. Gregson, M.D., Division of Infectious Diseases, 14-154 Warren Hall, Box 957119, Los Angeles, CA 90095. E-mail: a.gregson@ucla.edu

This article has an online supplement, which is accessible from this issue's table of contents at www.atsjournals.org

Am J Respir Crit Care Med Vol 192, Iss 12, pp 1490–1503, Dec 15, 2015

Copyright © 2015 by the American Thoracic Society

Originally Published in Press as DOI: 10.1164/rccm.201503-0558OC on August 26, 2015

Internet address: www.atsjournals.org

At a Glance Commentary

Scientific Knowledge on the

Subject: Acute allograft rejection (AR) was among the first identified risk factors for chronic lung allograft rejection (chronic lung allograft dysfunction) after lung transplantation. Although infections post-transplantation are common, AR is the single most pervasive event. As such, AR remains a leading risk factor for chronic lung allograft dysfunction, but the mechanisms underlying the evolution of AR into chronic lung allograft dysfunction are poorly understood.

What This Study Adds to the

Field: In this study, we validate bronchoalveolar lavage fluid exosomal shuttle RNA as a novel source for understanding the pathophysiology of allograft rejection and for biomarker discovery in lung transplantation. We show that exosomal shuttle RNA population signatures are distinctly different between patients with and without acute cellular rejection at the time of sample collection. Basal pulmonary metabolic pathways are overrepresented in quiescence, whereas AR samples demonstrated a skewed profile of antigen processing and both innate and adaptive immune activation. We have also identified novel upstream activation targets for potential therapeutic intervention and find that existing therapeutic agents may be beneficial in acute lung allograft rejection.

T cells (5). Although infections post-transplantation are common, AR is the single most pervasive event, with approximately 50% of most lung transplant programs' recipients experiencing at least one episode (6). As such, AR remains a leading risk factor for CLAD, but the mechanisms underlying the evolution of AR into CLAD are poorly understood.

AR detection requires invasive lung biopsy, which has poor sensitivity (7) and inherent risks (8). Because of this, intense surveillance for AR is limited, reducing early recognition. There is

treatment for AR, but not for CLAD, thus AR is treated to decrease the risk of subsequent CLAD, but its treatment increases the risk of infection and cancer. Therefore, blanket treatment of all transplant patients can paradoxically increase the risk of CLAD and cancer in those without AR.

Exosomes, which are 20- to 100-nm membrane vesicles derived from the multivesicular body with special lipid and protein composition, provide a mechanism for intercellular transfer of protected RNA and protein. On entry into the target cell, exosomes can modify the function of the recipient cell (9). As such, exosomes have been shown to alter cellular behavior in allergy (10), are capable of T-cell activation via both major histocompatibility class I and II and macrophages (11), have antiviral and antibacterial properties (12, 13), and promote angiogenesis (14).

We hypothesized that exosomal mRNA, or exosomal shuttle RNA (esRNA) (9), representing the bronchoalveolar lavage fluid (BALF) transcriptome could provide novel insights into allograft function during rejection and bacterial infections, such as with *Pseudomonas*. Improving the understanding of the underlying pathophysiology of AR may lead to novel interventions, perhaps with existing drugs that target pathways not yet recognized as important in AR and lung transplantation, but already in use for the treatment of cancer or other disorders.

Furthermore, because protected mRNA within exosomes reflects the

underlying state of their cellular source, biomarker discovery using exosomes may provide a sensitive and specific marker for acute rejection, leading to increased recognition of AR and decreased CLAD risk.

A biomarker based on esRNA could be easily translated to the clinical laboratory for same-day results. The goal of this study was to characterize the esRNA content using modern sequencing methods in a cohort of post-lung-transplant recipients with either stable allograft function or AR.

Methods

Patient Cohort

The cohort was constructed by the collection of consecutive BALF samples from different patients, each with greater than 20 ml of processed fluid that was free of microbial pathogens as determined by the clinical microbiology laboratory. The first 12 such samples were accepted for the study and were either free of lung allograft injury by transbronchial biopsy and spirometric decline (quiescent samples) or were associated with biopsy-proven AR.

BALF Preparation

BALF was isolated from patients who had received a lung transplant as previously reported (15). The collection and analysis of BALF and exosomes was approved by the UCLA Institutional Review Board. The

Table 1. Demographics of Patient Samples

Patient	Pretransplant Diagnosis	Transplant	Age (yr)	Sex
1	Pulmonary fibrosis	Double	53	F
2	Pulmonary fibrosis	Single	62	M
3	COPD, emphysema	Single	72	M
4	Pulmonary fibrosis	Single	53	F
5	Scleroderma	Double	50	M
6	Pulmonary fibrosis	Double	52	F
7	Pulmonary fibrosis	Single	65	F
8	COPD, emphysema	Single	62	F
9	Rheumatoid lung disease	Double	39	F
10	Graft failure, retransplant	Single	54	F
11	Cystic fibrosis	Double	44	M
12	Pulmonary fibrosis	Double	65	M

Definition of abbreviation: COPD = chronic obstructive pulmonary disease.

final volume of the BALF used for exosomal isolation varied between 20 and 60 ml.

Exosome Isolation

Exosomes were separated from BALF via ultracentrifugation (16). Briefly, BALF supernatant was run through low-speed ultracentrifugation at $12,000 \times g$ for 45

minutes at 4°C to pellet protein complexes and cellular/bacterial debris. The resultant supernatant was centrifuged at $100,000 \times g$ for 2 hours at 4°C to pellet the exosomes using a SW 41 Ti rotor (Beckman Coulter, Brea, CA). The exosome pellet obtained was then centrifuged again at $110,000 \times g$ for 1 hour at 4°C to clean pelleted exosomes.

This exosome pellet was resuspended in 60–120 μl phosphate-buffered saline buffer.

Flow Cytometry

The tetraspans (CD9, CD63, CD81) are the major exosome surface markers and were used to identify exosomes in the BALF by flow cytometry (17). Latex beads (Life Technologies, Carlsbad, CA) were coated with anti-CD63 (Invitrogen Corporation, Carlsbad, CA) antibody and incubated overnight with exosomes as previously described (18). Exosome-bead complexes were stained with fluorescent tagged anti-CD9 PE (EBiosciences, Inc., San Diego, CA) and anti-CD81 APC (EBiosciences, Inc.). Flow cytometry was performed on a standard FACSCalibur (BD Biosciences, San Jose, CA) and results analyzed in R/Bioconductor (19, 20). Representative results are shown in the online supplement.

RNA Extraction

We used miRNeasy (Qiagen, Hilden, Germany) and miRCURY (Exiqon, Vedbaek, Denmark) to isolate RNA from exosomes and BALF cellular pellets per manufacturers' instructions. Total RNA was paired-end sequenced using NuGen Ovation library construction (NuGen, San Carlos, CA). Bioanalysis was done on an Agilent 2100 using the Eukaryote Total RNA Pico Series II (Agilent, Santa Clara, CA) and RNA-Seq analysis on an Illumina HiSeqEquation 2500 Sequencing System (Illumina, San Diego, CA).

ELISA and Quantitative Polymerase Chain Reaction

ELISA kits for β -defensin-119 (MyBioSource catalog number MBS945365) and Deleted in Malignant Brain Tumor 1 (DMBT1; Biomatik catalog number EKU03679) were used to determine if these proteins were detectable in BALF. A DMBT1 primer (Life Tech catalog number 4,331,182) was used to determine if this transcript was present in BALF, with 18S used to normalize expression of DMBT1.

Statistical Analysis

All analysis was performed in R and Bioconductor (19, 20), with Limma processed data fed into Ingenuity Pathway Analysis (IPA) (www.ingenuity.com) for causal analysis (21). The genome was aligned to GRCh37 via Rsubread (22).

Table 2. Select Genes Overrepresented in Rejection Samples as Compared with Quiescent Samples

Gene Symbol	Gene Name	Log Fold Change	Adjusted P Value
DMBT1	Deleted in malignant brain tumors 1	4.04	6×10^{-5}
NOS1	Nitric oxide synthase 1	3.83	0.0002
CD1B	CD1b molecule	3.71	0.0004
CYP24A1	Cytochrome P450, family 24, subfamily A, polypeptide 1	5.14	0.0005
LDLR	LDL receptor	3.75	0.0005
IL33	Interleukin 33	-3.38	0.0005
C4A	Complement component 4A (Rogers Blood Group)	6.09	0.0007
PIK3C3	Phosphatidylinositol 3-kinase, catalytic subunit type 3	3.57	0.0007
COL11A1	Collagen, type XI, $\alpha 1$	3.83	0.0008
TLR2	Toll-like receptor 2	3.76	0.0008
MAP3K2	Mitogen-activated protein kinase 2+	3.71	0.0008
IL2RG	Interleukin 2 receptor- γ	6.42	0.0009
MAPK9	Mitogen-activated protein kinase 9	5.28	0.0009
EEA1	Early endosome antigen 1	-3.36	0.0009
JAK2	Janus kinase 2+	3.55	0.001
CD63	CD63 molecule (exosome related)	3.62	0.002
MYD88	Myeloid differentiation primary response 88	3.56	0.002
DPCR1	Diffuse panbronchiolitis critical region 1 (HLA-I)	3.43	0.002
OR2T3	Olfactory receptor, family 2, subfamily T, member 3	4.59	0.003
DEFB119	Defensin β 119	5.65	0.004
SFTPA2	Surfactant protein A2	5.13	0.004
IL6ST	Interleukin 6 signal transducer	3.69	0.004
IRF2	Interferon regulatory factor 2 (part of Jak-STAT path)	3.42	0.004
PDCD2	Programmed cell death 2	3.44	0.005
BECN1	Beclin 1 (autophagy related)	3.27	0.005
MIR1244-1	microRNA-1244-1	-2.65	0.005
CXCL16	Chemokine (C-X-C motif) ligand 16	-3.21	0.005
CISH	Cytokine inducible SH2-containing protein	3.61	0.009
TRGV5	T-cell receptor γ variable 5	5.12	0.015
OR8B3	Olfactory receptor, family 8, subfamily B, member 3	3.86	0.015
BAG4	BCL2-associated athanogene 4	2.91	0.04
CD36	CD36 (thrombospondin receptor) (exosome related)	-3.27	0.04
HLA-DPA1	HLA class II, DP $\alpha 1$	-3.58	0.05
CD37	CD37 molecule (exosome, tetraspanin)	4.75	0.06
FCGR2A	Fc fragment of IgG, low-affinity IIa receptor (CD32)	3.33	0.76

Limma was used as the primary analysis, with Voom transformation of the data using quantile normalization followed by group-means parameterization and robust eBayes (23). Gene-set enrichment analysis was performed using the Reactome pathways and the Generally Applicable Gene-set Enrichment, the latter without preprocessing via Limma (24). IPA Upstream Regulator Analysis was used to identify upstream regulators of the differentially expressed genes in our dataset and predict whether they were activated or inhibited.

Results

Patient Population

The median time in days of sample collection from transplantation was similar between those with ($n = 6$) and without ($n = 6$) AR (77 [interquartile range, 201] vs. 157 [832]; $P = 0.3$). The median AR score was 2. None of the samples had clinical or microbiologic evidence of infection or

colonization. The reason for lung transplantation included six who had pulmonary fibrosis, two with chronic obstructive pulmonary disease/emphysema, and one each with scleroderma, rheumatoid lung disease, cystic fibrosis, and graft failure. Six were double lung transplants, five were male, and the average age was 56 years (Table 1).

Individual Gene Targets

Because exosome RNA expression has not previously been evaluated in lung transplantation, we began an exploratory analysis, the goal of which was to describe the change in the lung allograft transcriptome that occurs during AR. The AR samples were skewed toward an inflammatory response involving pathways in both the innate and adaptive immune systems (Table 2; see Figure E10 in the online supplement). Additionally, many olfactory receptor genes were elevated, including *OR2T3*, *OR8B3*, *OR2A4*, *OR1N1*, *OR8 U1*, *OR2W1*, and *OR51A7*. Several genes elevated in the quiescent BALF

esRNA profile were underrepresented during rejection, including CXCL16, IL-33, and EEA-1 (see bottom of Table 2).

Gene-Set Analysis

Reactome pathway. A better understanding of the biology represented by the individual gene expression can be obtained via analysis of the functional networks or pathways that these genes form based on their biologic actions. Herein, we used the Reactome pathway database and Generally Applicable Gene-set Enrichment to identify networks that were overexpressed or underexpressed. The results of the Reactome pathway analysis were strikingly different between the quiescent esRNA and the AR esRNA. Barplots demonstrating Reactome pathways that were overrepresented in either quiescent BALF esRNA (Figure 1) or during acute rejection (Figure 2) are presented herein. The Reactome profile from overall BALF esRNA demonstrated a predominance of cellular communication and basal

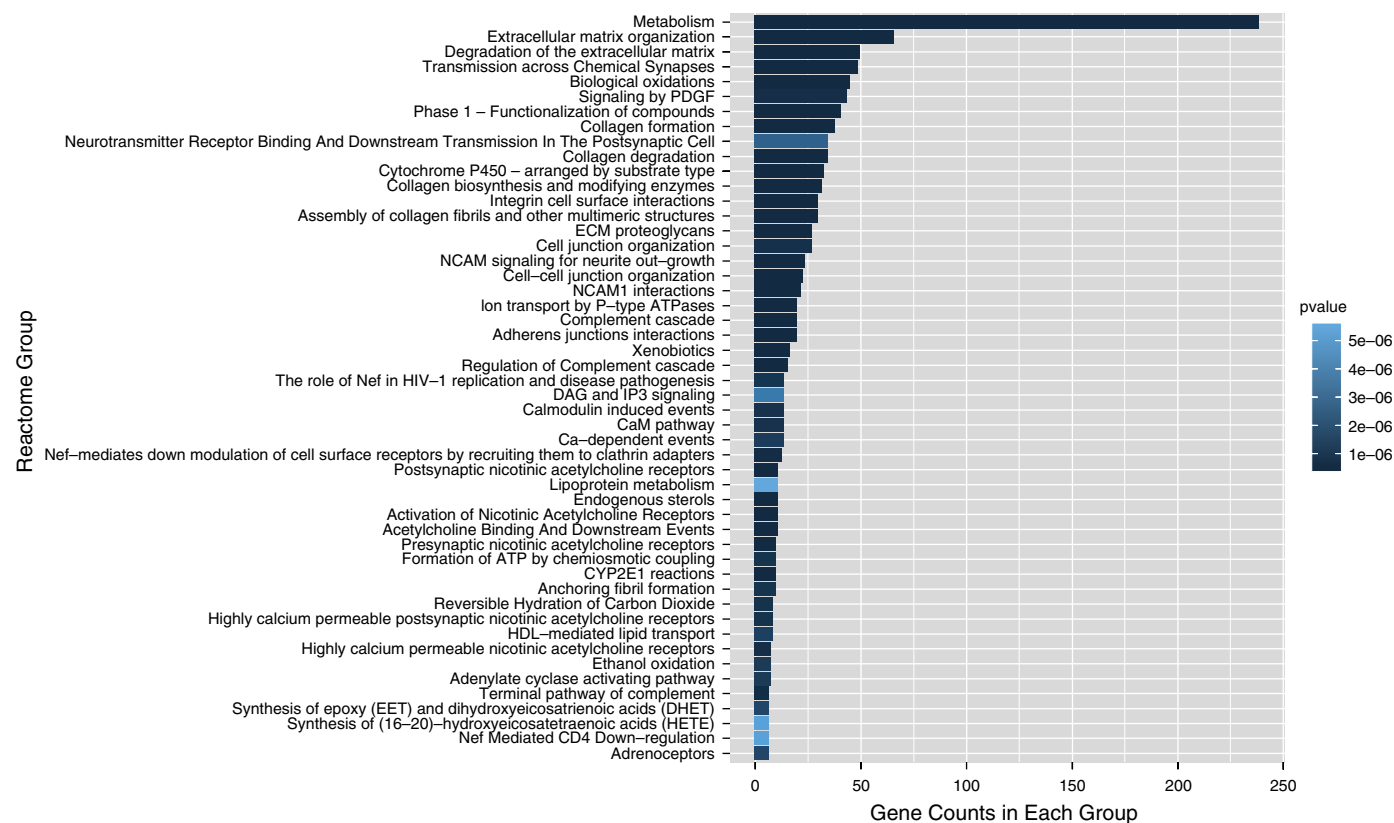


Figure 1. Quiescent-samples Reactome results for the bronchoalveolar lavage fluid exosomes analyzed by Limma group-means parameterization. The number of altered genes in a particular pathway is given on the x-axis.

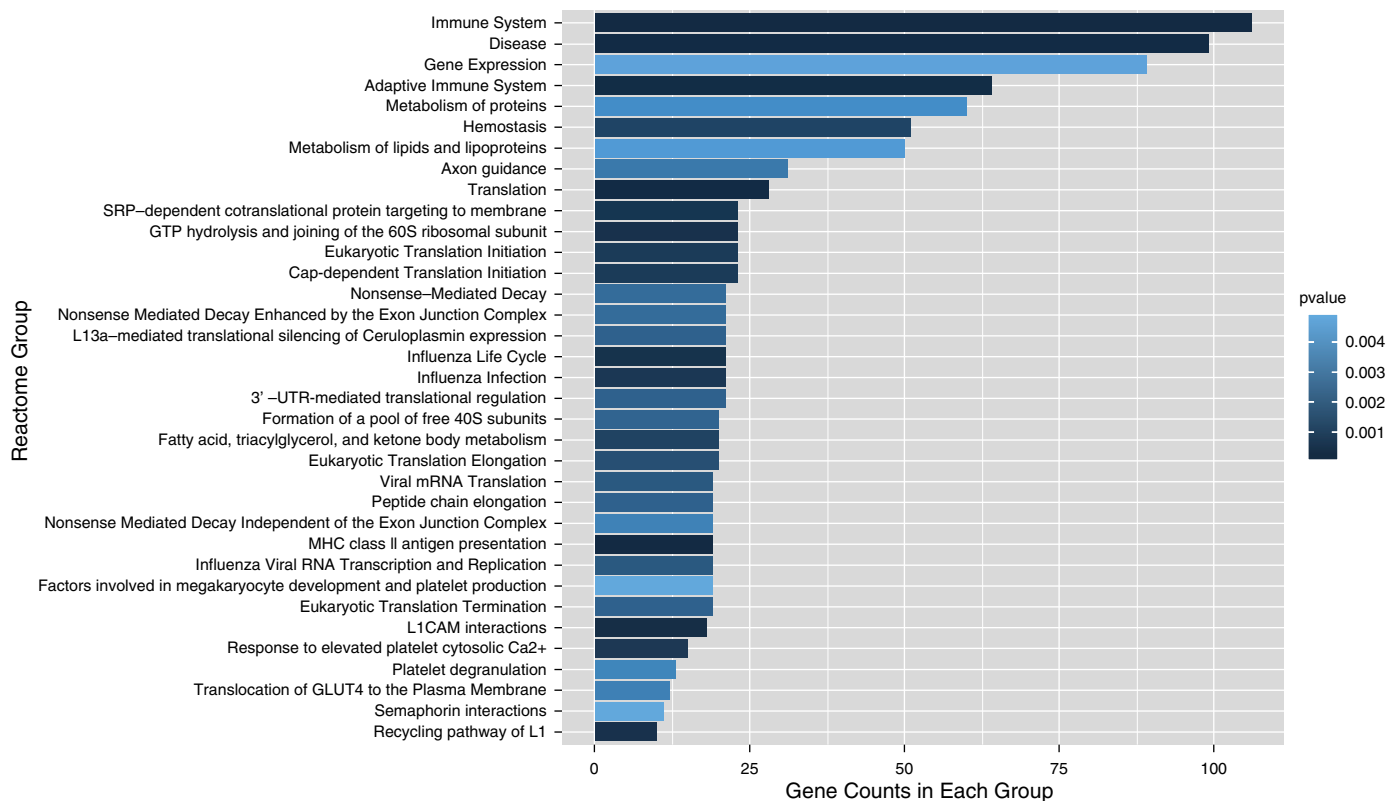


Figure 2. Reactome results for exosomes from acute rejection samples analyzed by Limma group-means parameterization. The number of altered genes in a particular pathway is given on the *x*-axis.

metabolism of the lung. Examples of this basal metabolism included the nicotinic acetylcholine receptor pathway, maintenance pathways of the extracellular matrix, platelet-derived growth factor signaling, and transmission across synapses. In the acute rejection samples, the up-regulated pathways were clearly skewed toward an inflammatory environment composed of both innate and adaptive immune responses with both major histocompatibility class I and II represented.

Kyoto Encyclopedia of Genes and

Genomes gene-set analysis. During AR Kyoto Encyclopedia of Genes and Genomes (KEGG) gene-set analysis found activation of both innate and adaptive immune pathways. Overrepresented innate gene sets included cytokine signaling (IL-1 β , IL-6, and IL-18 in particular), complement activation, and TGF, VEGF, Wnt, and notch signaling, as well as natural killer cell pathways including NOD-like receptors, natural killer cell-mediated cytotoxicity, and more generally genes associated with leukocyte transendothelial migration. T- and B-cell gene sets were well represented by B-cell receptor

signaling, Fc receptor phagocytosis, protein processing in the ER, MAPK, mTOR, and Jak-STAT signaling. A reductive approach to these gene sets to reduce overlap of up-regulated genes is shown in Table 3, and the entire gene set can be seen in Table E6. Representative diagrams of up- and down-regulated gene sets are shown for natural killer cell signaling (Figure 3) and MAP kinase pathways (see Figure E11).

Causal Analysis

Although the gene-set analysis provides for functional grouping of genes, the causal analysis attempts to identify pathways enriched based on known interactions, and can describe potential upstream regulators. The IPA causal analysis of differentially expressed genes during AR identified EIF-2, Sertoli cell junction, and hypoxia signaling to be the top three canonical pathways (Figure 4). As can be seen in Table 4, numerous pathways associated with both innate and adaptive immunity, cell proliferation and differentiation, apoptosis, tissue injury, and repair are enriched by

genes overexpressed during AR (see Table E7). The Rac signaling canonical pathway overlaps significantly with the EIF-2 pathway and is central to many adaptive immune functions of importance in lung allograft rejection. Putative upstream regulators of these pathways and genes are seen in Table 5 (see Table E8). Top upstream regulators by *P* value of overlap with genes in the esRNA include the transcriptional regulators TP53 (*z* score, 0.71), ERG (*z* score, -1.16), mir-32 (no *z* score), IL13 (*z* score, 1.73), and SNRK (no *z* score). Other potential upstream regulators include luteinizing hormone (*z* score, -2.24), the metalloprotease MMP2 (*z* score, 1.52), growth hormone (*z* score, 1.28), follicle-stimulating hormone (*z* score, -2.00), mir-124-3p (*z* score, -2.00), insulin-like growth factor binding protein 2 (*z* score, 2.00) and PI3K (*z* score, 1.53). Many of these regulators are important for normal cell cycle function, and as a consequence, abnormal function has often been identified in cancers, thus the frequent associations in our analysis with them in cancers. Many

Table 3. Essential Kyoto Encyclopedia of Genes and Genomes Gene Sets as Determined by Generally Applicable Gene-set Enrichment, Using a Reductive Approach

Essential Gene Sets	q Value	Set Size
hsa03010 ribosome	7×10^{-39}	90
hsa04510 focal adhesion*	2×10^{-23}	200
hsa04520 adherens junction	3×10^{-15}	73
hsa04145 phagosome	4×10^{-15}	150
hsa04144 endocytosis	6×10^{-13}	201
hsa04141 protein processing in endoplasmic reticulum	6×10^{-13}	166
hsa04530 tight junction	2×10^{-11}	130
hsa04360 axon guidance	2×10^{-11}	128
hsa04910 insulin signaling pathway	2×10^{-10}	136
hsa04722 neurotrophin signaling pathway	2×10^{-10}	125
hsa03013 RNA transport [†]	4×10^{-8}	151
hsa04070 phosphatidylinositol signaling system [‡]	5×10^{-8}	77
hsa04962 vasopressin-regulated water reabsorption	5×10^{-8}	43
hsa04670 leukocyte transendothelial migration	9×10^{-8}	113
hsa04114 oocyte meiosis	3×10^{-7}	111
hsa04120 ubiquitin-mediated proteolysis	4×10^{-7}	136
hsa04612 antigen processing and presentation	1×10^{-6}	69
hsa04380 osteoclast differentiation	1×10^{-6}	126
hsa04142 lysosome	2×10^{-6}	121
hsa03040 spliceosome	3×10^{-6}	127
hsa03050 proteasome	8×10^{-5}	44
hsa04110 cell cycle	0.0001	125
hsa04150 mTOR signaling pathway	0.0002	51
hsa00010 glycolysis/gluconeogenesis	0.0003	64
hsa03008 ribosome biogenesis in eukaryotes	0.0003	78
hsa04914 progesterone-mediated oocyte maturation	0.0003	84
hsa00190 oxidative phosphorylation	0.0004	118
hsa04210 apoptosis	0.0006	87
hsa00480 glutathione metabolism	0.0006	50
hsa03018 RNA degradation	0.0007	71
hsa04710 circadian rhythm—mammal	0.001	23
hsa04260 cardiac muscle contraction	0.001	72
hsa04320 dorsoventral axis formation	0.001	24
hsa02010 ABC transporters	0.001	44
hsa04610 complement and coagulation cascades	0.002	69
hsa00310 lysine degradation	0.002	44
hsa04350 TGF- β signaling pathway	0.003	83
hsa04640 hematopoietic cell lineage	0.003	84
hsa00640 propanoate metabolism	0.004	32
hsa00230 purine metabolism	0.004	160
hsa04621 NOD-like receptor signaling pathway	0.004	57
hsa00620 pyruvate metabolism	0.004	40
hsa04330 Notch signaling pathway	0.004	47
hsa04514 cell adhesion molecules	0.005	129
hsa04920 adipocytokine signaling pathway	0.007	68
hsa03060 protein export	0.008	23
hsa03320 PPAR signaling pathway	0.008	70
hsa00052 galactose metabolism	0.01	27
hsa00020 citrate cycle (TCA cycle)	0.01	30
hsa00970 aminoacyl-tRNA biosynthesis	0.01	41
hsa00071 fatty acid metabolism	0.01	43
hsa00330 arginine and proline metabolism	0.01	53
hsa04976 bile secretion	0.02	71
hsa00280 valine, leucine, and isoleucine degradation	0.02	44
hsa04630 Jak-STAT signaling pathway	0.02	153

The reductive approach removes overlapping genes from gene sets and pools them together into the most frequently represented gene sets.

*Other included groups: hsa04510 focal adhesion, hsa04810 regulation of actin cytoskeleton, hsa04666 Fc- γ R-mediated phagocytosis, hsa04720 long-term potentiation, hsa04010 MAPK signaling pathway, hsa04512 ECM-receptor interaction, hsa04012 ErbB signaling pathway, hsa04662 B-cell receptor signaling pathway, hsa04270 vascular smooth muscle contraction, hsa04660 T-cell receptor signaling pathway, hsa04971 gastric acid secretion, hsa04730 long-term depression, hsa04912 GnRH signaling pathway, hsa04310 Wnt signaling pathway, hsa04540 gap junction, hsa04970 salivary secretion, hsa04020 calcium signaling pathway, hsa04973 carbohydrate digestion and absorption, hsa04972 pancreatic secretion, hsa04062 chemokine signaling pathway, hsa04960 aldosterone-regulated sodium reabsorption, hsa04916 melanogenesis, hsa04664 Fc epsilon RI signaling pathway, hsa04370 VEGF signaling pathway, and hsa04974 protein digestion and absorption.

[†]hsa03013 RNA transport and hsa03015 mRNA surveillance pathway.

[‡]hsa04070 phosphatidylinositol signaling system, hsa00562 inositol phosphate metabolism, and hsa00561 glycerolipid metabolism.

therapies are designed for cancer, including at least one now used in transplantation, bortezomib.

Comparison with Cellular Pellet Transcriptome

Comparison of the esRNA transcriptome with that of the cellular pellet was done to determine if there were significant differences between these two sources of RNA. Eleven of the same 12 samples used for esRNA extraction were available for cellular pellet RNA-Seq analysis, from here on termed “RNA-p.” There was a striking difference between the two RNA populations, with the RNA-p populations extremely biased toward T- and B-cell-associated products. Among the top five individual genes in the RNA-p were CXCL13, T-cell receptor β variable 5–5, and CTLA4 (see Table E9). An IPA analysis of RNA-p found that T-cell receptor signaling, CCR5 signaling in macrophages, and CTLA4 signaling in CD8 T cells were the top three canonical pathways (see Table E10). Top upstream regulators for RNA-p included the T-cell receptor (z score, 2.15), CD3 (z score, -2.54), IL21 (z score, 1.81), CD28 (z score, -2.14), and interferon- γ (z score, 2.96) (see Table E11).

A comparison analysis in IPA between esRNA and RNA-p demonstrated a probable T-cell bias of the RNA-p. For example, the canonical pathway of Tec kinase was predicted to be up-regulated during AR in both esRNA and RNA-p, but a Tec (ITK, IL2-inducible T-cell kinase) is seen only in the RNA-p, whereas the genes involved in the pathway from the esRNA analysis included JAK2 and STAT5B. CTLA4 signaling provided another example with TRAT1 (a TCR-associated molecule) and ZAP70 (the zeta TCR chain) only appearing in the RNA-p, not the esRNA. This was a common theme in the concordant pathways. Discordant pathways chemokine signaling, leukocyte extravasation signaling, and sperm motility were predicted down-regulated in esRNA and up-regulated in RNA-p, whereas type 1 diabetes signaling was predicted up in esRNA and down in RNA-p. RNA for CD8, CD38, and multiple chemokines and cytokines were abundant in the RNA-p, but missing from the esRNA. Overlapping upstream regulators were identified based on z score, those being IL13 (esRNA

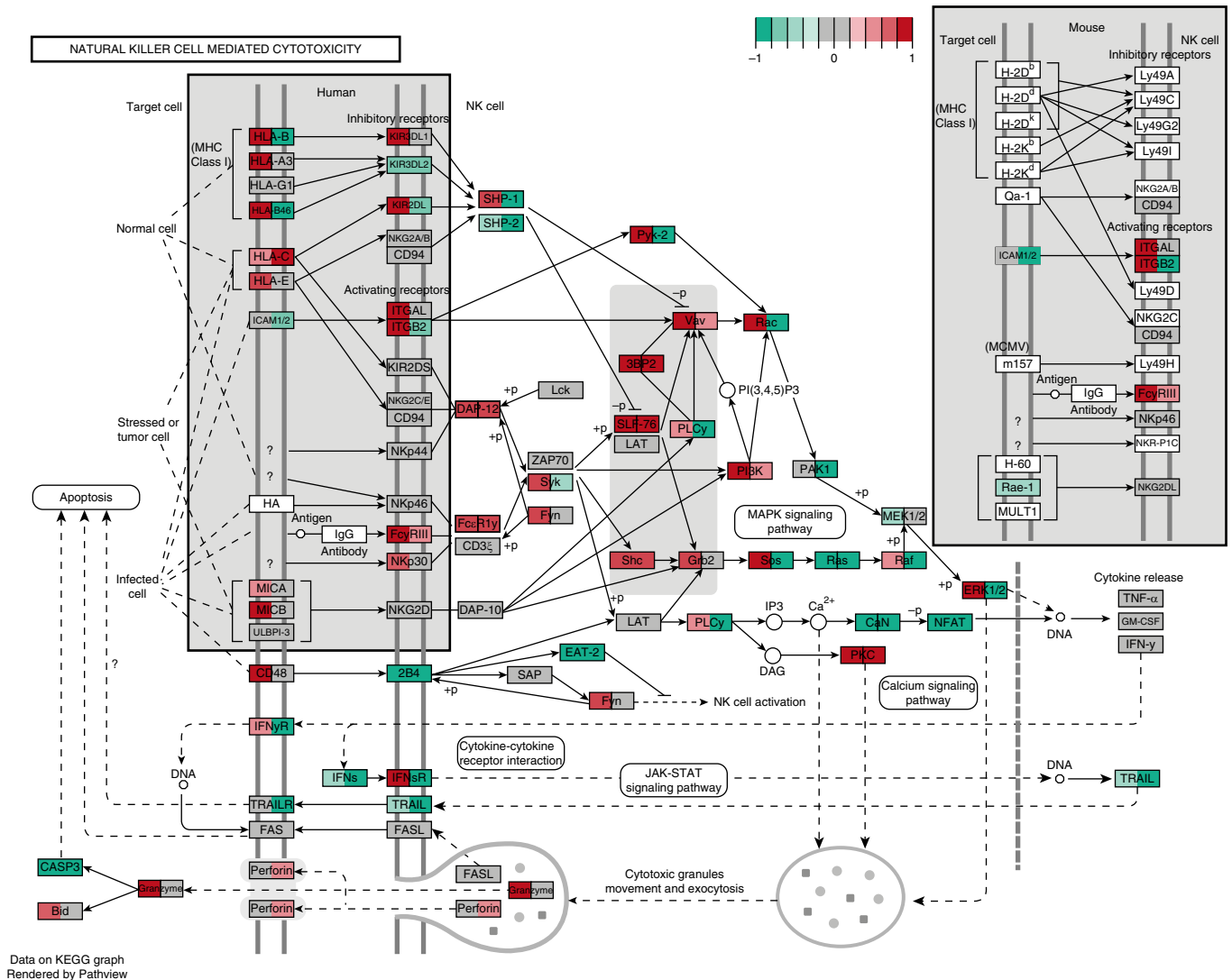


Figure 3. Example pathway from Generally Applicable Gene-set Enrichment Kyoto Encyclopedia of Genes and Genomes analysis of exosomal shuttle RNA. Representative example of natural killer cell-mediated cytotoxicity comparing rejection (*left*) and quiescent (*right*) conditions.

predicted up and RNA-p down) and PI3K, TP53, PIM1, and NR3C1 (esRNA and RNA-p both predicted up), but again the downstream regulated products differed between esRNA and RNA-p and with many more downstream products identified in the esRNA.

Discussion

This study presents the first in-depth analysis of the BALF esRNA population after lung transplantation and is the first to evaluate for differential expression between AR and quiescence. The esRNA transcriptome is distinctly different from

the cellular pellet transcriptome and allows access to a unique allograft compartment not previously studied. We show that esRNA population signatures are distinctly different between patients with and without AR at the time of sample collection. Basal pulmonary metabolic pathways are overrepresented in quiescence, whereas AR samples demonstrated a skewed profile of antigen processing and both innate and adaptive immune activation. We have also identified novel upstream activation targets for potential therapeutic intervention and find that existing therapeutic agents may be beneficial in AR. These findings validate

BALF esRNA as a source for understanding the pathophysiology of AR and for biomarker discovery in lung transplantation.

The quiescent, post-transplant BALF esRNA profile consisted of metabolic pathways critical to basic lung function, such as collagen biosynthesis, platelet-derived growth factor signaling, cell surface interactions, complement cascade, and nicotinic acetylcholine receptor messaging. Intracellular vesicular trafficking gene transcripts were highly overrepresented including those with endosomal (*EEA1*) and Golgi origin (*TRAPPC11*, *GOLM1*), and the synaptogamins, which help to mediate trafficking in a calcium-dependent manner

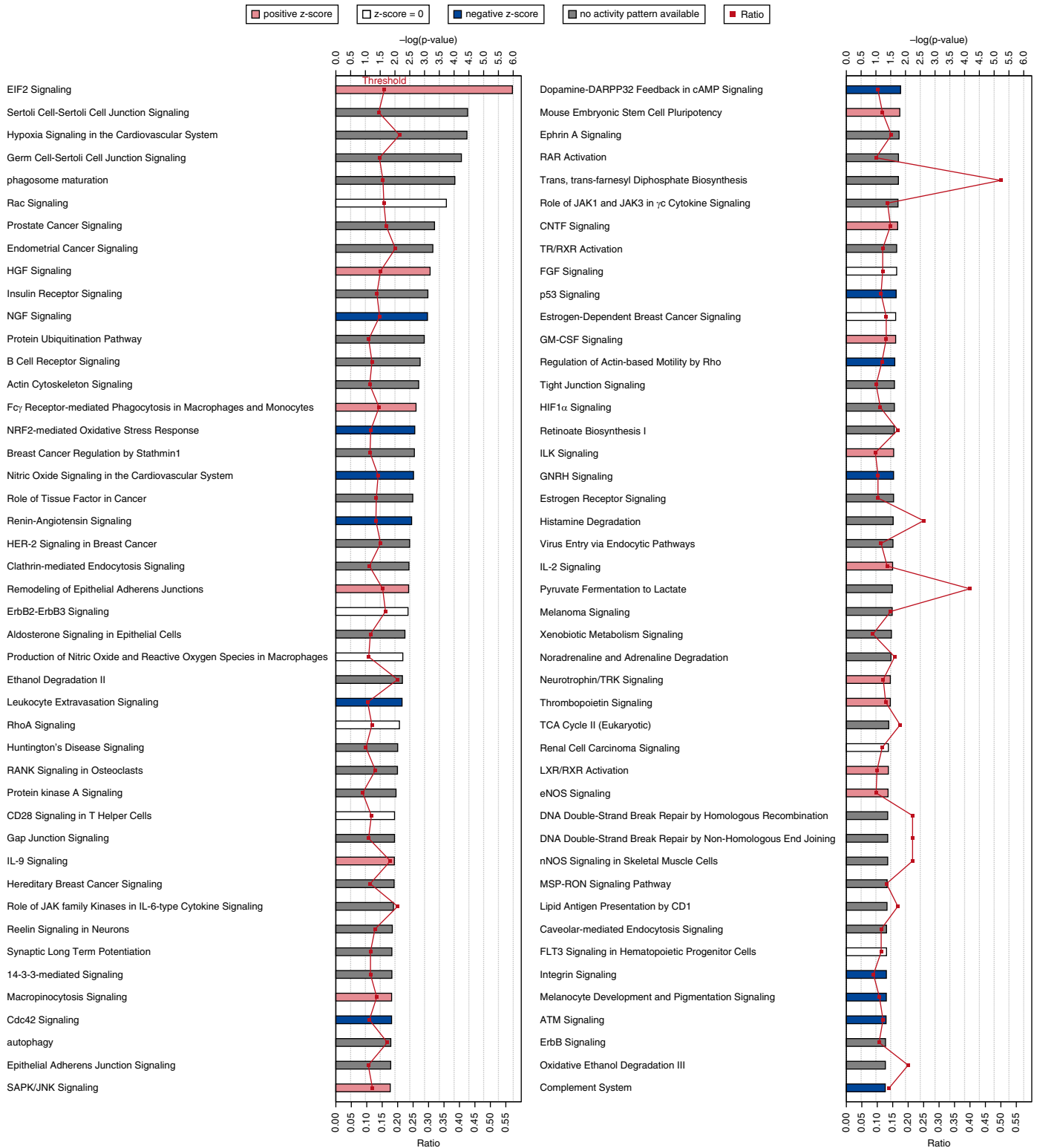


Figure 4. Ingenuity Pathway Analysis canonical pathways enriched by genes differentially expressed in acute cellular rejection samples in exosomal shuttle RNA.

Table 4. Top Ingenuity Pathway Analysis Canonical Pathway List by *P* Value for esRNA

Canonical Pathway	−log(<i>P</i> Value)	Ratio	<i>z</i> Score	Molecules
EIF2 signaling	5.97	0.157	0.471	EIF2S1, GSK3B, RPL32, RPL37A, RPL35A, RPL23, PIK3R1, RPL27, RPL5, RPL38, RPS15A, RPL37, RPL3, PIK3C3, RPS25, EIF3A, ATM, INSR, RPL13, EIF5, RPL24, RPS9, EIF2AK4, PPP1CB, RPS4X, RPS15, RPL27A
Sertoli cell–Sertoli cell junction signaling	4.46	0.139		GSK3B, ATF2, MAP3K5, PTEN, DLG1, TJP1, MLLT4, CTNNB1, YBX3, AXIN1, TUBB8, PRKAG2, TUBA1C, PRKAR1A, SPTBN1, TUBB2A, TUBA1A, NOS1, MAP3K2, ITGB1, MAP3K1, TUBA1B, MAP3K4, MAPK9
Hypoxia signaling in the cardiovascular system	4.44	0.206		ATF2, PTEN, ATM, UBE2D3, UBE2D4, BIRC6, UBE2V2, LDHA, CREBBP, UBE2Q1, MDM2, HSP90AA1, UBE2R2
Germ cell–Sertoli cell junction signaling	4.25	0.141		LIMK2, MAP3K5, TJP1, MLLT4, CTNNB1, PAK1, ATM, AXIN1, TUBB8, PIK3R1, TUBA1C, RHOA, TUBB2A, TUBA1A, GSN, MAP3K2, ITGB1, MAP3K1, TUBA1B, MAP3K4, MAPK9, PIK3C3
Phagosome maturation	4.03	0.153		DYNC1H1, DYNC1I2, BET1L, B2M, PIKFYVE, TUBB8, TUBA1C, VPS39, TUBB2A, GPAA1, TUBA1A, NOS1, ATP6V0A1, EEA1, TUBA1B, LAMP2, ATP6V0E1, PIK3C3
Rac signaling	3.74	0.155	0	ACTR2, LIMK2, PAK1, ATM, TIAM1, PIKFYVE, PIK3R1, ARPC1B, ACTR3, RHOA, PTK2B, CYFIP1, ITGB1, MAP3K1, PRKCI, PIK3C3
Prostate cancer signaling	3.34	0.163		GSK3B, ATF2, PTEN, NKX3-1, CTNNB1, ATM, PIK3R1, CCND1, CREBBP, MDM2, GSTP1, HSP90AA1, PIK3C3
Endometrial cancer signaling	3.28	0.192		GSK3B, PTEN, CTNNB1, CCND1, ATM, ERBB2, AXIN1, MLH1, PIK3R1, PIK3C3
HGF signaling	3.19	0.144	0.258	ATF2, MAP3K5, PAK1, ATM, PIK3R1, RAP1A, PTPN11, MAP3K2, ITGB1, MAP3K1, CCND1, PRKCI, MAP3K4, MAPK9, PIK3C3
Insulin receptor signaling	3.11	0.133		GSK3B, PTEN, JAK2, VAMP2, ATM, INSR, PRKAG2, PIK3R1, PRKAR1A, PPP1R10, PTPN11, PPP1CB, ACLY, ASIC2, PRKCI, STX4, PIK3C3
NGF signaling	3.1	0.142	−0.258	ATF2, MAP3K5, ATM, PIK3R1, RAP1A, RHOA, PTPN11, RPS6KA2, MAP3K2, MAP3K1, TRIO, CREBBP, MAP3K4, MAPK9, PIK3C3
Protein ubiquitination pathway	2.99	0.106		DNAJA1, PSMD11, USP36, FBXW7, DNAJC21, UBE2V2, DNAJC15, PSMC1, PSMD2, HSP90AA1, UBE2R2, DNAJC30, PSMA4, B2M, UBE2D3, DNAJB5, DNAJC8, UBE2D4, HSPA9, USP9X, USP2, HSPA5, BIRC6, UCHL3, UBE2Q1, MDM2, USP38
B-cell receptor signaling	2.85	0.117		GSK3B, ATF2, PAG1, MAP3K5, PTEN, CALM1 (includes others), ATM, PIK3R1, RAP1A, FCGR2A, PTK2B, PTPN11, MAP3K2, MAP3K1, CREBBP, IGHG3, MAP3K4, MAPK9, PIK3C3, VAV3
Actin cytoskeleton signaling	2.8	0.11		ACTR2, LIMK2, PAK1, ATM, EZR, ARHGAP35, MSN, TIAM1, PIKFYVE, PIK3R1, ARPC1B, ACTR3, MYH9, RHOA, PFN1, GSN, CYFIP1, ITGB1, TRIO, PPP1CB, PIK3C3, TMSB10/TMSB4X, VAV3
Fc-γ receptor-mediated phagocytosis in macrophages and monocytes	2.71	0.14	1.387	ACTR2, PTEN, PAK1, EZR, PIK3R1, ARPC1B, ACTR3, FCGR2A, PTK2B, PRKCI, YES1, ARF6, VAV3
NRF2-mediated oxidative stress response	2.67	0.113	−1.89	DNAJA4, GSK3B, GSTA5, DNAJA1, MAP3K5, ABCC4, ATM, PIK3R1, DNAJB5, DNAJC8, DNAJC21, MAP3K1, DNAJC15, CREBBP, PRKCI, GSTP1, CUL3, MAPK9, PIK3C3, NFE2L2
Breast cancer regulation by Stathmin1	2.66	0.111		LIMK2, CALM1 (includes others), UHMK1, RB1CC1, PAK1, ATM, TUBB8, PRKAG2, PIK3R1, TUBA1C, RHOA, PRKAR1A, TUBB2A, TUBA1A, PPP1R10, ITPR3, TUBA1B, PPP1CB, ITPR1, PRKCI, PIK3C3
Nitric oxide signaling in the cardiovascular system	2.63	0.137	−0.277	CACNA1E, CALM1 (includes others), ATM, ATP2A2, PRKAG2, PIK3R1, PRKAR1A, ITPR3, CACNA1C, ITPR1, PRKCI, HSP90AA1, PIK3C3

(Continued)

Table 4. (Continued)

Canonical Pathway	−log(P Value)	Ratio	z Score	Molecules
Role of tissue factor in cancer	2.6	0.131		LIMK2, PTEN, JAK2, PAK1, ATM, PIK3R1, FRK, PTK2B, PTPN11, RPS6KA2, ITGB1, STAT5B, YES1, PIK3C3
Renin–angiotensin signaling	2.56	0.13	−0.535	ATF2, JAK2, PAK1, ATM, PRKAG2, PIK3R1, PRKAR1A, ITPR3, PTK2B, MAP3K1, ITPR1, PRKCI, MAPK9, PIK3C3
HER-2 signaling in breast cancer	2.5	0.145		GSK3B, MAP3K5, ITGB1, CCND1, ATM, ERBB2, PRKCI, MDM2, PIK3R1, ERBB3, PIK3C3
Clathrin-mediated endocytosis signaling	2.47	0.109		ACTR2, CLTC, ATM, AP2B1, PIK3R1, APOC1, ARPC1B, ACTR3, NUMB, LYZ, USP9X, LDLR, PICALM, SH3GLB1, ITGB1, SERPINA1, MDM2, ARF6, STAM, PIK3C3
Remodeling of epithelial adherens junctions	2.46	0.152	0.447	TUBB2A, TUBA1A, ACTR2, CTNBN1, TUBA1B, TUBB8, TUBA1C, ARF6, ACTR3, ARPC1B
ErbB2–ErbB3 signaling	2.44	0.161		GSK3B, PTEN, CCND1, ATM, ERBB2, PIK3R1, ERBB3, STAT5B, PIK3C3
Aldosterone signaling in epithelial cells	2.34	0.113		DNAJC30, DNAJA1, ATM, PIKFYVE, PIK3R1, DNAJB5, DNAJC8, HSPA9, DNAJC21, ITPR3, DNAJC15, HSPA5, ASIC2, ITPR1, PRKCI, HSP90AA1, PIK3C3
Production of nitric oxide and reactive oxygen species in macrophages	2.27	0.106	0	MAP3K5, JAK2, ATM, PIK3R1, APOC1, RAP1A, RHOA, LYZ, PPP1R10, MAP3K2, MAP3K1, PPP1CB, SERPINA1, CREBBP, PRKCI, MAP3K4, TLR2, MAPK9, PIK3C3
Ethanol degradation II	2.25	0.2		ADH7, ALDH1A2, ADH1C, ALDH1A1, ACSS2, ADH4

Definition of abbreviation: esRNA = exosomal shuttle RNA.

The ratio is the number of differentially expressed genes from our data that map to the Ingenuity Pathway Analysis pathway, divided by the total number of genes that exist in that canonical pathway. A positive z score predicts that the activation state is “activated,” whereas a negative value predicts that the activation state is “inhibited.” If there are too few overlapping genes or if the number of overlapping genes is not consistent in the predicted direction, then the z score is not resulted.

(25). This is probably a reflection of our exosomal source of RNA. Such a profile is in agreement with prior work that demonstrated a nonunique transcriptome core across a broad range of tissues consisting largely of intracellular components (26).

During rejection, components of innate immunity including complement, surfactants, defensins, TLR2, MYD88, and nitric oxide synthase were all elevated. Among these, most interesting was the finding of overrepresentation of DMBT1 in rejection. DMBT1 provides important links between inflammation, innate immunity, infection, and cancer (27). *DMBT1* encodes for secreted scavenger molecules with cysteine-rich domains that act as pattern recognition receptors (28). *DMBT1* can act like surfactants and bind directly to microbial pathogens, initiate aggregation, and thereby reduce epithelial cell invasion (29). In fact, *DMBT1* may be more important for agglutination of *Streptococcus mutans* than is secretory IgA, with which *DMBT1* also engages in a calcium-dependent mechanism (30). *DMBT1* can also interact with surfactant A, leading to alveolar macrophage migration (31), and it is up-regulated by type I interferons and LPS (29).

Of even greater significance to lung transplantation, *DMBT1* was recently found to promote endothelial cell migration, proliferation, and angiogenesis via interactions with VEGF, suggesting a possible mechanism for progression from AR to fibrosis and CLAD (32).

β-Defensins were also found to be overexpressed in esRNA during AR, echoing studies showing up-regulation in rat models of acute lung injury (33) and in human samples of bronchiolitis obliterans syndrome (34). β-Defensins can interact with both TLR1 and TLR2, the latter of which was elevated in our rejection samples. Interestingly, TLR2 mRNA expression was previously found to be increased in monocytes and biopsy specimens from patients with grade 3A cardiac rejection (35), and studies of renal (36) and liver (37) rejection, suggesting a role for it in allograft rejection. Also up-regulated in rejection samples were PIK3C3 and Beclin-1. Both are integral to macroautophagy, an important process to remove damaged proteins and mitochondria from cells, and to TLR9 signaling (38). Up-regulation of these innate immune genes points to the possibility that infection post-

transplantation is an upstream, initiating event for acute rejection. Another possibility is that this up-regulation in AR primes the allograft toward exaggerated innate defenses, facilitating the progression from acute to chronic rejection, when AR is followed by an infection, such as *Pseudomonas*, *Staphylococcus*, or *Aspergillus* (39–41).

Gene-set analysis of AR samples showed marked differences from quiescent samples, with an overall shift toward immune and disease state activation. In rejection, the Reactome pathways of adaptive immune system, translation, HLA class II presentation, and membrane transport mechanisms were all increased. KEGG gene-set analysis showed that HLA-I (and MICB) activation was associated with increased KIR expression in rejection. This in turn could lead to increased γ-interferon and granzyme production (Figure 3). Potential migration of these activated lymphocytes into the graft is seen via expression of genes associated with chemotaxis and invasion, such as CXCR4 and the MMPs, as demonstrated in the KEGG analysis.

Table 5. Selected Upstream Regulators from Ingenuity Pathway Analysis for esRNA

Upstream Regulator	Molecule Type	z Score	P Value	Target Molecules in Dataset
TP53	Transcription regulator	0.707	0.0000952	ADRBK2, ARL6IP1, ARPC1B, ATF3, BCL2L11, BHLHE40, BTG2, CHD3, CTNNB1, CTSD, DAPK1, DGKA, DLG1, ERCC1, FBXW7, FDF1, FDPS, FUBP1, GSK3B, HK2, HMG2, LATS2, LDHA, LIMK2, MAP4, MCM3, MDM2, MLF2, MLH1, OMA1, PEG10, PLK2, PTEN, PTP4A1, PTPN11, RB1CC1, RPS25, SCN3B, SEMA3C, SPATA18, TBL1X, TJP1, TMSB10/TMSB4X, TPX2, TRIO, VCAN, XPC, YES1
IL13	Cytokine	1.73	0.000463	ABCA1, ALDH1A2, ATF3, BZW2, C3, CD1B, CD36, CD37, CISH, CXCR2, EPAS1, GPX3, GSN, KCNJ15, LTA4H, MS4A4A, MUC2, RFTN1, RPS6KA2, SLC26A6, TIMP4
ERG	Transcription regulator	-1.155	0.000506	APOC1, ARHGAP31, CDK5RAP2, CTNNB1, DOCK10, DOCK2, FLNB, FLNC, FMNL3, NUMB, PHACTR2, PRKCI, PTPN11, RYR3, SVIL, TACC1, TRIOBP
miR32	MicroRNA		0.000542	BCL2L11, BTG2, MDM2
SNRK	Kinase		0.000542	CACYBP, CCND1, CTNNB1
Lh	Complex	-2.236	0.00129	ACTR2, ARHGAP35, ATP2A2, ATP1F1, BECN1, DAPK1, EZR, FLNC, HK2, ITPR1, JMJD6, MAP3K5, MAP4K4, MAPK6, NPC2, PRKAR1A, PTP4A1, SRD5A2, TLK1, TUBA1A, TYRO3, YBX3
MMP2	Peptidase	1.522	0.00239	CCND1, IL2RG, IL6ST, JAK2, TJP1
TCF/LEF	Group		0.00271	CCND1, ITGB1
PPARD	Ligand-dependent nuclear receptor	-0.796	0.00306	FABP3, PDK4, PPARD, PTEN, YWHAE
Growth hormone	Group	1.276	0.00311	CCND1, CISH, KLF10, LDLR, PDK4, PLK2, PRKAG2, ZEB2
FSH	Complex	-2	0.00358	ACTR2, ARHGAP35, ATP2A2, ATP1F1, BECN1, BTG2, DAPK1, EZR, FLNC, HK2, ITPR1, JMJD6, KLF10, LDLR, MAP3K5, MAP4K4, MAPK6, NPC2, PRKAR1A, PTP4A1, STX4, TLK1, TUBA1A, TYRO3, YBX3
TP73	Transcription regulator	-0.661	0.00558	BHLHE40, COX411, CTNNB1, DLG1, MCM3AP, MDM2, N4BP2L2, PLK2, PNR1, PTPN3, RB1CC1, SERPINA1, TBL1X, TRIM32
Estrogen receptor	Group	0.03	0.00619	ABCA1, ABCG1, ABCG2, C3, CALB2, CCND1, DSC2, ERBB2, ERBB3, FGFR2, FLNC, HSP90AA1, ITGB1, KLF10, MSN, PCDH19, TIMP2, TIMP4, WNT5B
miR-124-3p	Mature microRNA	-2	0.00629	ATP6V0E1, ELOVL5, LAMC1, SERP1
RBM5	Other	-1.504	0.00722	BTG2, CASP10, HSP90AA1, MLH1, MYO1B, STAT5B, UCP2
PI3K (family)	Group	1.526	0.01	ABCA1, ABCG1, BCL2L11, HSPA5, ITGB1, NFE2L2, SLC4A7, TJP1
MAP2K1/2	Group	0.692	0.01	ATF3, BCL2L11, C3, CCND1, HK2, HSPA5
NDRG1	Kinase	0.132	0.0101	ATF3, BCL2L11, CCND1, CTNNB1
E2F1	Transcription regulator		0.0106	ABCG2, BCL2L11, CALM1 (includes others), CCND1, GPS2, MAP3K5, MCM3, MEIS1, MLH1, NCL, PRKDC, PRPSAP1, RBBP8, STAM, YBX3, YWHAE
A2M	Transporter	1	0.0125	CCND1, GSK3B, HSPA5, MAP3K5
MMP9	Peptidase		0.0128	CCND1, ITGB1, TJP1
ERBB2	Kinase	1.236	0.0162	BHLHE40, CCND1, DZIP3, ERBB2, ERBB3, GSK3B, IL6ST, ITGB1, KRT81, LAMP2, MDM2, MPHOSPH9, MSMB, NET1, TUBA1A, WNT5B
AR	Ligand-dependent nuclear receptor	1.308	0.0178	ABCA1, ABCG4, ABCG1, ACTR3, CTNNB1, ERBB2, LMOD1, MYO1B, NKX3-1, PROS1, PTHLH, VCAN
MGEA5	Enzyme	0.229	0.0234	ACSS2, CALB1, CCND1, CNOT1, CTNNB1, ERBB3, FDF1, FDPS, FLNB, GNE, HRNR, KRT81, LRIG1, PDCD2, PHKB, STARD4, TIMP2, TSPAN12, TUBA1A
INS	Other	0.692	0.0237	ACLY, CD36, COX411, CUL5, INSR
PIM1	Kinase	1.044	0.0294	ERBB2, ERBB3, INSR, MDM2
NEDD9	Other	-1.342	0.0301	AOAH, BHLHE40, MKNK2, PLAC8, PPP1R3B
CEBPB	Transcription regulator	1.082	0.0309	ALDH1A1, C3, CCND1, CDC42EP3, DAPK1, FGFR2, INSR, SAA2
IGFBP2	Other	2	0.0387	COL11A1, MALAT1, PTEN, RBMS3

(Continued)

Table 5. (Continued)

Upstream Regulator	Molecule Type	z Score	P Value	Target Molecules in Dataset
LDL	Complex	-0.351	0.0415	ABCA1, C3, CD36, CTNNA1, HSPA5
NR3C1	Ligand-dependent nuclear receptor	0.447	0.0438	ABHD2, BAG4, BCL2L11, BHLHE40, BRWD1, CAPN2, CASP10, CDC42EP3, DNAJC15, DUSP22, ELMOD3, FASTKD2, JMJD6, LGALS8, MAGI3, MAPK9, MYD88, NMT1, NSMAF, PAK1, PIK3R1, PLK2, PRKAR1A, PRKCI, PTK2B, RBMS3, RTN4, SH3GLB1
HMGA1	Transcription regulator	0.45	0.0439	ATM, CCND1, IDI1, INSR
mir-34	Microrna	-0.283	0.0439	AHCYL1, CCND1, CPLX2, PPP1R10
RAB1B	Other	2	0.0828	DERL1, RHOBTB3, SEC31A, SERP1
MDM2	Transcription regulator	1.982	0.0906	CCND1, HIST2H2BE, LYZ, MDM2
IgG	Complex	-1.89	0.392	B2M, EZR, HSPA5, KLK11, LDLR, TRIM16, TUBB2A
PDLIM2	Other	2	1	CLCN4, DNAJC15, MECOM, OAS3

Definition of abbreviation: esRNA = exosomal shuttle RNA.

P value is the P value of overlap. z score is "activation z score." A positive z score predicts that the activation state is "activated," whereas a negative value predicts that the activation state is "inhibited." If there are too few overlapping genes or if the number of overlapping genes is not consistent in the predicted direction, then the z score is not resulted.

We also used an alternative approach to gene-set analysis: causal pathway analysis, which leverages the directional changes in gene expression within the data set with anticipated upstream and downstream regulatory pathways. Examination of two top canonical pathways by causal analysis, EIF-2 and Rac signaling, identified potential novel drug interventions acting on PI3K, AKT, c-RAF, and MEK. One such drug, bortezomib, is already in use in transplantation targeting antibody-mediated rejection in renal and liver transplantation (42) and graft-versus-host disease (43), the latter perhaps via an IL-6-dependent mechanism (44), a pathway elevated in our rejection samples as seen by IL6ST. Bortezomib has also been shown to reduce levels of MMP9, an upstream pathway in our analysis (45). Importantly, the IPA analysis allowed us to identify an upstream cluster of genes, which can help us to better understand the pathogenesis of AR. Using this approach we identified a novel upstream regulator cluster of TP73/TP53, FSH/LH, PI3K, ERG, MMP2/9, E2F1/E2F6, and TCF/LEF. In addition to their possible use as early warning biomarkers, these genes may also be substantially valuable therapeutic targets for preventing AR or CLAD. Many of these targets deserve evaluation both *in vitro* and in preclinical animal models of rejection.

Although we did not specifically target miRNA with our RNA-Seq analysis, we did find several miRNA overexpressed in quiescent post-lung-transplant exosomes, including the

miRNA548 family that is hypothesized to interact with an extremely wide variety of cellular processes including focal adhesion, regulation of the actin cytoskeleton, and tight junctions to name a few, all of which are of importance in normal lung biology. miRNA548i may also down-regulate expression of type III interferons during viral infection and therefore be important in host defense and inflammation within the lung (46). miRNA367 is deregulated weeks after bleomycin-induced pulmonary damage and is predicted to interact with the transforming growth factor- β pathway, suggesting a possible connection with fibrosis and CLAD (47).

Immune profiling in lung transplantation has relied primarily on downstream protein production (39, 48) and cellular analysis (7, 15, 49–51). It is possible that up-regulated immune/inflammatory genes seen at the time of AR are not primarily responsible for the initiation of AR; therefore, they may not be suitable biomarkers if the purpose of the biomarker discovery is to detect the onset of AR before an uncontrollable immune activation takes place. As a method of immune profiling, esRNA transcriptomic analysis illuminates not only individual genes, but entire pathways and upstream regulators, providing a fuller picture of the underlying pathology and allowing for identification of potential upstream targets to prevent injury before onset of significant inflammation.

Our comparison with the cellular pellet transcriptome shows that esRNA represents a unique compartment within the lung allograft that provides information not obtainable from the cellular pellet. It is possible that transcripts found within the esRNA population could have been found in the RNA-p if the adaptive immune response were not so vigorous, in effect drowning out the detection of other transcripts. Although we cannot be sure of the source of the esRNA, it is clearly distinct from the cellular pellet RNA-p. The inclusion of transcripts, such as *DMBT1* and *SLPI*, suggests but does not prove that the esRNA source contains a significant population of allograft epithelial cells.

The BALF esRNA provides a unique window into the pathogenesis of AR. Up-regulation of the genes in our AR cohort clearly illustrates the onset of a severe inflammatory environment, which most likely participates in the acute allograft rejection even in the presence of potent immunosuppressive drugs. Novel upstream pathways associated with rejection could provide an early warning mechanism to impending rejection and identifiable targets for pharmacologic intervention in acute lung allograft rejection. ■

Author disclosures are available with the text of this article at www.atsjournals.org.

Acknowledgment: The authors are grateful to the patients for their participation in this study and for the dedicated clinical care provided by their physicians. They also thank Dr. Rosal Mendez and Xochitl Gonzalez, M.F.A., for their thoughtful editorial assistance.

References

- Bando K, Paradis IL, Similo S, Konishi H, Komatsu K, Zullo TG, Yousem SA, Close JM, Zeevi A, Duquesnoy RJ, et al. Obliterative bronchiolitis after lung and heart-lung transplantation. An analysis of risk factors and management. *J Thorac Cardiovasc Surg* 1995;110:4–13, discussion 13–14.
- Al-Githmi I, Batawil N, Shigemura N, Hsin M, Lee TW, He G-W, Yim A. Bronchiolitis obliterans following lung transplantation. *Eur J Cardiothorac Surg* 2006;30:846–851.
- Verleden GM, Raghu G, Meyer KC, Glanville AR, Corris P. A new classification system for chronic lung allograft dysfunction. *J Heart Lung Transplant* 2014;33:127–133.
- Burton CM, Carlsen J, Mortensen J, Andersen CB, Milman N, Iversen M. Long-term survival after lung transplantation depends on development and severity of bronchiolitis obliterans syndrome. *J Heart Lung Transplant* 2007;26:681–686.
- Gelman AE, Li W, Richardson SB, Zinselmeyer BH, Lai J, Okazaki M, Kornfeld CG, Kreisel FH, Sugimoto S, Tietjens JR, et al. Cutting edge: acute lung allograft rejection is independent of secondary lymphoid organs. *J Immunol* 2009;182:3969–3973.
- Snell GI, Westall GP, Paraskeva MA. Immunosuppression and allograft rejection following lung transplantation: evidence to date. *Drugs* 2013;73:1793–1813.
- Greenland JR, Jewell NP, Gottschall M, Trivedi NN, Kukreja J, Hays SR, Singer JP, Golden JA, Caughey GH. Bronchoalveolar lavage cell immunophenotyping facilitates diagnosis of lung allograft rejection. *Am J Transplant* 2014;14:831–840.
- Glanville AR. The role of surveillance bronchoscopy post-lung transplantation. *Semin Respir Crit Care Med* 2013;34:414–420.
- Valadi H, Ekström K, Bossios A, Sjöstrand M, Lee JJ, Lötvall JO. Exosome-mediated transfer of mRNAs and microRNAs is a novel mechanism of genetic exchange between cells. *Nat Cell Biol* 2007;9:654–659.
- Levänen B, Bhakta NR, Torregrosa Paredes P, Barbeau R, Hiltbrunner S, Pollack JL, Sköld CM, Svartengren M, Grunewald J, Gabrielsson S, et al. Altered microRNA profiles in bronchoalveolar lavage fluid exosomes in asthmatic patients. *J Allergy Clin Immunol* 2013;131:894–903.e8.
- Bhatnagar S, Schorey JS. Exosomes released from infected macrophages contain *Mycobacterium avium* glycopeptidolipids and are proinflammatory. *J Biol Chem* 2007;282:25779–25789.
- Kesimer M, Scull M, Brighton B, DeMaria G, Burns K, O'Neal W, Pickles RJ, Sheehan JK. Characterization of exosome-like vesicles released from human tracheobronchial ciliated epithelium: a possible role in innate defense. *FASEB J* 2009;23:1858–1868.
- Timár CI, Lorincz AM, Csepányi-Kömi R, Vályi-Nagy A, Nagy G, Buzás EI, Iványi Z, Kittel A, Powell DW, McLeish KR, et al. Antibacterial effect of microvesicles released from human neutrophilic granulocytes. *Blood* 2013;121:510–518.
- Janowska-Wieczorek A, Wysoczynski M, Kijowski J, Marquez-Curtis L, Machalinski B, Ratajczak J, Ratajczak MZ. Microvesicles derived from activated platelets induce metastasis and angiogenesis in lung cancer. *Int J Cancer* 2005;113:752–760.
- Gregson AL, Hoji A, Palchevskiy V, Hu S, Weigt SS, Liao E, Derhovanessian A, Saggari R, Song S, Elashoff R, et al. Protection against bronchiolitis obliterans syndrome is associated with allograft CCR7+ CD45RA- T regulatory cells. *PLoS One* 2010;5:e11354.
- Théry C, Amigorena S, Raposo G, Clayton A. Isolation and characterization of exosomes from cell culture supernatants and biological fluids. *Curr Protoc Cell Biol* 2006;Chapter 3:Unit 3.22.
- Rubinstein E, Le Naour F, Lagaudrière-Gesbert C, Billard M, Conjeaud H, Boucheix C. CD9, CD63, CD81, and CD82 are components of a surface tetraspan network connected to HLA-DR and VLA integrins. *Eur J Immunol* 1996;26:2657–2665.
- Lässer C, Eldh M, Lötvall J. Isolation and characterization of RNA-containing exosomes. *J Vis Exp* 2012;59:e3037.
- R Development Core Team. R: a language and environment for statistical computing [2009; accessed 2015 Nov 13]. Available from: <http://www.R-project.org>
- Gentleman RC, Carey VJ, Bates DM, Bolstad B, Dettling M, Dudoit S, Ellis B, Gautier L, Ge Y, Gentry J, et al. Bioconductor: open software development for computational biology and bioinformatics. *Genome Biol* 2004;5:R80.
- Krämer A, Green J, Pollard J Jr, Tugendreich S. Causal analysis approaches in ingenuity pathway analysis. *Bioinformatics* 2014;30:523–530.
- Liao Y, Smyth GK, Shi W; Y L. The Subread aligner: fast, accurate and scalable read mapping by seed-and-vote. *Nucleic Acids Res* 2013;41:e108.
- Smyth GK. Limma: linear models for microarray data. In: Gentleman R, Carey V, Dudoit S, Irizarry R, Huber W, editors. *Bioinformatics and computational biology solutions using R and bioconductor*. New York: Springer; 2005. pp. 397–420.
- Luo W, Friedman MS, Shedden K, Hankenson KD, Woolf PJ. GAGE: generally applicable gene set enrichment for pathway analysis. *BMC Bioinformatics* 2009;10:161.
- Hou JC, Min L, Pessin JE. Insulin granule biogenesis, trafficking and exocytosis. *Vitam Horm* 2009;80:473–506.
- Ramsköld D, Wang ET, Burge CB, Sandberg R. An abundance of ubiquitously expressed genes revealed by tissue transcriptome sequence data. *PLoS Comput Biol* 2009;5:e1000598.
- Müller H, End C, Weiss C, Renner M, Bhandiwad A, Helmke BM, Gassler N, Hafner M, Poustka A, Mollenhauer J, et al. Respiratory Deleted in Malignant Brain Tumours 1 (DMBT1) levels increase during lung maturation and infection. *Clin Exp Immunol* 2008;151:123–129.
- Holmskov U, Mollenhauer J, Madsen J, Vitved L, Gronlund J, Tornøe I, Kliem A, Reid KB, Poustka A, Skjold K. Cloning of gp-340, a putative opsonin receptor for lung surfactant protein D. *Proc Natl Acad Sci USA* 1999;96:10794–10799.
- Rosenstiel P, Sina C, End C, Renner M, Lyer S, Till A, Hellmig S, Nikolaus S, Fölsch UR, Helmke B, et al. Regulation of dMBT1 via nOD2 and tLR4 in intestinal epithelial cells modulates bacterial recognition and invasion. *J Immunol* 2007;178:8203–8211.
- Rundegren J, Arnold RR. Differentiation and interaction of secretory immunoglobulin A and a calcium-dependent parotid agglutinin for several bacterial strains. *Infect Immun* 1987;55:288–292.
- Tino MJ, Wright JR. Glycoprotein-340 binds surfactant protein-A (SP-A) and stimulates alveolar macrophage migration in an SP-A-independent manner. *Am J Respir Cell Mol Biol* 1999;20:759–768.
- Müller H, Hu J, Popp R, Schmidt MHH, Müller-Decker K, Mollenhauer J, Fisslthaler B, Eble JA, Fleming I. Deleted in malignant brain tumors 1 is present in the vascular extracellular matrix and promotes angiogenesis. *Arterioscler Thromb Vasc Biol* 2012;32:442–448.
- Liu K-X, Chen S-Q, Zhang H, Guo JY, Li Y-S, Huang W-Q. Intestinal ischaemia/reperfusion upregulates beta-defensin-2 expression and causes acute lung injury in the rat. *Injury* 2009;40:950–955.
- Ross DJ, Cole AM, Yoshioka D, Park AK, Belperio JA, Laks H, Strieter RM, Lynch JP III, Kubak B, Ardehali A, et al. Increased bronchoalveolar lavage human beta-defensin type 2 in bronchiolitis obliterans syndrome after lung transplantation. *Transplantation* 2004;78:1222–1224.
- McDaniel DO, Zhou X, Moore CK, Aru G. Cardiac allograft rejection correlates with increased expressions of Toll-like receptors 2 and 4 and allograft inflammatory factor 1. *Transplant Proc* 2010;42:4235–4237.
- Hoffmann U, Bergler T, Rihm M, Pace C, Krüger B, Jung B, Reinhold SW, Farkas S, Rümmele P, Krämer BK, et al. Impact of Toll-like receptor 2 expression in renal allograft rejection. *Nephrol Dial Transplant* 2011;26:1080–1087.
- Deng J-F, Geng L, Qian Y-G, Li H, Wang Y, Xie H-Y, Feng X-W, Zheng S-S. The role of toll-like receptors 2 and 4 in acute allograft rejection after liver transplantation. *Transplant Proc* 2007;39:3222–3224.
- O Farrell F, Rusten TE, Stenmark H. Phosphoinositide 3-kinases as accelerators and brakes of autophagy. *FEBS J* 2013;280:6322–6337.
- Gregson AL, Wang X, Weigt SS, Palchevskiy V, Lynch JP III, Ross DJ, Kubak BM, Saggari R, Fishbein MC, Ardehali A, et al. Interaction between *Pseudomonas* and CXC chemokines increases risk of bronchiolitis obliterans syndrome and death in lung transplantation. *Am J Respir Crit Care Med* 2013;187:518–526.

40. Weigt SS, Copeland CAF, Derhovanessian A, Shino MY, Davis WA, Snyder LD, Gregson AL, Sagggar R, Lynch JP III, Ross DJ, *et al.* Colonization with small conidia *Aspergillus* species is associated with bronchiolitis obliterans syndrome: a two-center validation study. *Am J Transplant* 2013;13:919–927.
41. Gregson AL, Wang X, Injean P, Weigt SS, Shino M, Sayah D, DerHovanessian A, Lynch JP III, Ross DJ, Sagggar R, *et al.* Staphylococcus via an interaction with the ELR+ CXC chemokine ENA-78 is associated with BOS. *Am J Transplant* 2015;15:792–799.
42. Eskandary F, Bond G, Schwaiger E, Kikic Z, Winzer C, Wahrmann M, Marinova L, Haslacher H, Regele H, Oberbauer R, *et al.* Bortezomib in late antibody-mediated kidney transplant rejection (BORTEJECT Study): study protocol for a randomized controlled trial. *Trials* 2014; 15:107.
43. Herrera AF, Kim HT, Bindra B, Jones KT, Alyea EP III, Armand P, Cutler CS, Ho VT, Nikiforow S, Blazar BR, *et al.* A phase II study of bortezomib plus prednisone for initial therapy of chronic graft-versus-host disease. *Biol Blood Marrow Transplant* 2014;20:1737–1743.
44. Pai C-CS, Chen M, Mirsoian A, Grossenbacher SK, Tellez J, Ames E, Sun K, Jagdeo J, Blazar BR, Murphy WJ, *et al.* Treatment of chronic graft-versus-host disease with bortezomib. *Blood* 2014;124: 1677–1688.
45. Tiriveedhi V, Upadhya GA, Busch RA, Gunter KL, Dines JN, Knolhoff BL, Jia J, Sarma NJ, Ramchandran S, Anderson CD, *et al.* Protective role of bortezomib in steatotic liver ischemia/reperfusion injury through abrogation of MMP activation and YKL-40 expression. *Transpl Immunol* 2014;30:93–98.
46. Li Y, Xie J, Xu X, Wang J, Ao F, Wan Y, Zhu Y. MicroRNA-548 down-regulates host antiviral response via direct targeting of IFN- λ 1. *Protein Cell* 2013;4:130–141.
47. Xie T, Liang J, Guo R, Liu N, Noble PW, Jiang D. Comprehensive microRNA analysis in bleomycin-induced pulmonary fibrosis identifies multiple sites of molecular regulation. *Physiol Genomics* 2011;43:479–487.
48. Neujahr DC, Uppal K, Force SD, Fernandez F, Lawrence C, Pickens A, Bag R, Lockard C, Kirk AD, Tran V, *et al.* Bile acid aspiration associated with lung chemical profile linked to other biomarkers of injury after lung transplantation. *Am J Transplant* 2014;14:841–848.
49. Hodge G, Hodge S, Reynolds PN, Holmes M. Airway infection in stable lung transplant patients is associated with decreased intracellular T-helper type 1 pro-inflammatory cytokines in bronchoalveolar lavage T-cell subsets. *Transpl Infect Dis* 2008;10:99–105.
50. Gregson AL, Hoji A, Sagggar R, Ross DJ, Kubak BM, Jamieson BD, Weigt SS, Lynch JP III, Ardehali A, Belperio JA, *et al.* Bronchoalveolar immunologic profile of acute human lung transplant allograft rejection. *Transplantation* 2008;85:1056–1059.
51. Neujahr DC, Cardona AC, Ulukpo O, Rigby M, Pelaez A, Ramirez A, Gal AA, Force SD, Lawrence EC, Kirk AD, *et al.* Dynamics of human regulatory T cells in lung lavages of lung transplant recipients. *Transplantation* 2009;88:521–527.